



## UAV swarm coordination based on parallel control

Journal:	<i>IEEE Transactions on Cybernetics</i>
Manuscript ID	CYB-E-2022-04-1040
Manuscript Type:	Regular Paper
Date Submitted by the Author:	25-Apr-2022
Complete List of Authors:	Li, Jiacheng; Unmanned Systems Technology Research Institute, Northwestern Polytechnical University Fang, Yangwang ; Unmanned System Research Institute, Northwestern Polytechnical University Ma, Wenhui; School of Automation, Northwestern Polytechnical University Wu, Zihao; Northwestern Polytechnical University School of Astronautics, Northwestern Polytechnical University Huangfu, shuaiqi; Unmanned Systems Technology Research Institute, Northwestern Polytechnical University yu, dengxiu; Northwestern Polytechnical University, Unmanned System Research Institute; University of Macau, Faculty of Science and Technology Chen, C.I.; University of Macau, the Faculty of Science and Technology
Keywords:	UAV Swarm, Parallel control, Turning, Obstacle Avoidance, Prescribed-time convergence, Bijection transform

SCHOLARONE™  
Manuscripts

# UAV swarm coordination based on parallel control

Jiacheng Li , Yang Wang Fang , Wenhui Ma , Zihao Wu , Shuaiqi Huangfu  Dengxiu Yu , Member, IEEE, and C. L. Philip Chen  Fellow, IEEE

**Abstract**—In this paper, to address the coordination problem about turning and obstacle avoidance for large-scale unmanned aerial vehicle (UAV) swarm, a novel parallel control method based on the transformation of time-domain and space-domain is proposed. Firstly, a large-scale UAV swarm is divided into the leadership and the followership based on the strategy of hierarchical grouping, which the leadership is composed of the swarm leader and the co-leader in each group and the followership is composed of the followers from different groups. Secondly, the control laws of the leaders and followers are designed where a time-varying scaling function is incorporated into the potential field functions, which can achieve the convergence of swarm system within a prescribed time. Then, to realize the swarm coordination via changing the relative position between UAVs, the bijection transform is introduced, which is a mapping between the real and virtual space-domain. Finally, simulation results show the collision-free turning and formation changes of the large-scale UAV swarm can be achieved effectively and rapidly.

**Index Terms**—UAV Swarm; Parallel control; Turning; Obstacle Avoidance; Prescribed-time convergence; Bijection transform.

## I. INTRODUCTION

WITH the development of multi-UAV technology in the military and civilian fields, the swarm control methods have attracted considerable attention of many scholars [1]–[4], especially for the control issues related to obstacle avoidance, formation transformation (composition, split, reconstruction), turning, system convergence time, etc [5]–[9].

To solve the problem of collision avoidance between UAVs [10], [11], the commonly used methods can be divided into the rule-based, optimization-based, strategy-coordination-based, and swarm-intelligence-based [12]. On this basis, some intelligent control methods such as neural network control, adaptive control, reinforcement learning control were also applied in collision avoidance [13]–[19]. Refs. [15] and [16] were both based on potential field function for obstacle avoidance control, which method reduces the amount of system calculation and make the swarm has high flexibility and reliability while ensures no collision of each UAV. A distributed collision

This work was supported by the National Natural Science Foundation of China (61973253). (Corresponding author: C. L. Philip Chen).

J. Li, Y. Fang, S. Huangfu and D. Yu are with Unmanned System Research Institute, Northwestern Polytechnical University, Xian 710072, China (e-mail: jiacheng\_li@mail.nwpu.edu.cn, ywfang@nwpu.edu.cn, yudengxu@nwpu.edu.cn, hfsq@mail.nwpu.edu.cn ).

W. Ma is with School of Automation, Northwestern Polytechnical University, Xian 710072, China (e-mail: mawenhuai.qiu@foxmail.com).

Z. Wu is with School of Astronautics, Northwestern Polytechnical University, Xian 710072, China (e-mail: wulaoker47@163.com).

C. L. Philip Chen is with the School of Computer Science and Engineering, South China University of Technology, Guangzhou 510641, China, and also with the College of Navigation, Dalian Maritime University, Dalian 116026, China (e-mail: philip.chen@ieee.org).

Manuscript received April 19, 2021; revised August 16, 2021.

avoidance strategies for UAV swarm over fixed and switching topologies was proposed in Ref. [17], which is useful in the swarm control due to its low energy consumption and computational cost. Besides, Ref. [18] introduced a distributed reinforcement learning approach into the swarm control, which has high application scalability to larger swarm via achieve context-awareness and implicitly coordinate the swarm's actions.

For large-scale UAVs control, it is difficult to achieve high-level autonomy for the swarm by only relying on obstacle avoidance control, which needs to combine the formation control techniques [19], [20]. Common formation control techniques include leader-follower method [15], virtual structure method and so on [21]–[26]. A key issue in formation control is to realize the swarm turning through formation transformation, which is also the embodiment of the swarm's self-adaptive and self-organizing [23]. At present, the rigid body turns [24]–[27] is a popular method for the swarm turning control whereas the peripheral UAVs need to be continuously accelerated to maintain the formation, which increases the energy consumption of the system and the distribution and scheduling of the system is uneven under this strategy. Inspired by the flight of birds [28], some scholars had proposed a turning strategy of democratic groups, that is, any member of the group can initiate a movement that other members will follow [29]. However, the disadvantage of this strategy is that when any UAV in the swarm fails, the whole swarm will be affected by it and fail the flight.

Furthermore, convergence within a specific time is necessary for swarm control because many practical formation tasks have timing requirements [30]–[34]. Especially for large-scale swarm, the fast convergence is necessary for swarm collision-free flight [35]–[40]. An observer-based adaptive fixed-time formation control method was proposed in Ref. [37], which can address the time-varying formation tracking problem via utilizing fixed-time non-smooth back-stepping technique. Ref. [38] proposed a distributed finite-time formation control methods, which solves the problem for multi-UAVs with collision avoidance and input saturation. In addition, to further improve the formation efficiency, the prescribed-time convergence control was introduced into the UAVs control [7], [39]. Unlike finite-time control, the convergence time of the prescribed-time control system can be specified from any initial state. A control method of distributed prescribed-time convex optimization for continuous-time multi-agent system was proposed in Ref. [40], which is possible to pre-assign the settling time arbitrarily according to task requirements.

From what has been discussed earlier, it can be found that although the researches on obstacle avoidance, forma-

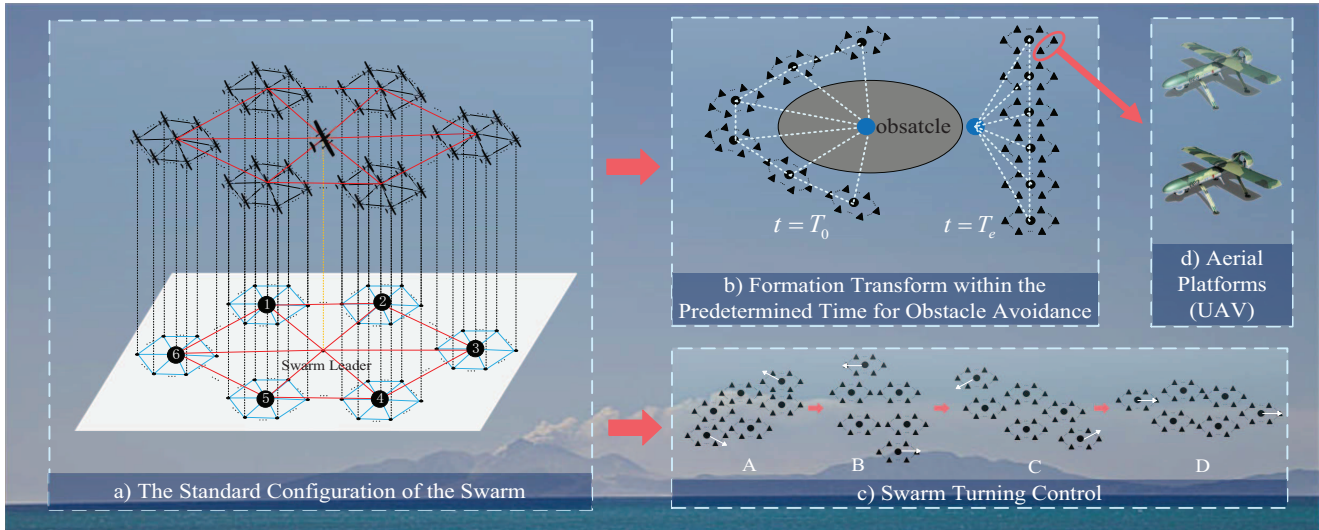


Fig. 1. Framework of the overall swarm system: In this paper, our control goal can be expressed in the following three aspects: i) The standard configuration of the swarm is inspired by the bird flock, which can be regarded as a round solid whole and even understood as a sphere. Based on the configuration of the swarm in the block diagram a), the computational complexity of the swarm is reduced during formation transformation, and the turning efficiency is improved. ii) When the swarm encounters a large obstacle, the Co-leader can adjust the swarm formation based on the bijective transformation to safely bypass the obstacle without collision within the prescribed-time( $T_{pre} = T_e - T_0$ ), which is as shown in the block diagram b). iii) The block diagram c) shows the transformation trend of each group during the swarm turning process. By adjusting the position of some UAVs, the turning of the whole swarm within the specified time is realized, in which improves the turning efficiency.

tion control and prescribe time control for the swarm have made some achievements, research on the simultaneous consideration of these controls are still insufficient, especially the research on dynamic coordinated obstacle avoidance and formation control for large-scale UAVs [41]. With the number of groups increases, the computational complexity and control requirements of the system also increase. That is to say, it is still a great challenge to build a highly autonomous swarm system in a predetermined time frame with great performance and robustness by using the existing research methods [42]–[44], especially for the large-scale system.

Fortunately, we have noticed that the parallel control proposed in Ref. [45]–[47] has a good solution to such large-scale and complex control problems, which basic idea is expanding the practical problems into virtual space and solving the problem by means of virtual-reality interaction. However, to the best of our knowledge, studies about this method have rarely used into the flight control system and its application problem up to now. Therefore, inspired by this method, a novel control method for UAV swarm to coordinate based on the parallel control is proposed in this paper. The framework is described in Fig. 1 and the contributions of this article are:

- 1) The parallel control based on the multiple feedback and large closed loop is introduced into the large-scale and complex swarm system control, which the virtual-real interaction, parallel drive and parallel execution are adopted to complete the control of swarm systems. Specifically, the swarm control law of the standard configuration is transformed in the time and space domain, respectively and simultaneously, to realize the arbitrary and stable transformation of the swarm in a prescribed time.
- 2) The hierarchical grouping control structure is adopted to

the large-scale swarm. Then, the standard configuration for the swarm is also constructed accordingly based on the designed structure. In this way, the partial or full transformation of the swarm can be achieved via adjusting the UAVs of different levels.

- 3) For the coordination problem of large-scale UAV swarm, the control strategy based on the bijection transformation is proposed, which the high-efficiency turn and obstacle avoidance of the large-scale swarm can be achieved within the prescribed time.

The structure of this paper is organized as follows: Notations and some basics about a swarm UAVs are introduced in section II. The cooperative control laws within the prescribed-time convergence for the swarm UAVs are designed in Section III. The control strategy for the swarm UAVs turning based on the bijection transform is designed in Section IV. In Section V, some numerical simulations are carried out to show the correctness of the proposed method. Section VI provides the conclusions of this study.

## II. PRELIMINARY AND PROBLEM FORMULATION

In this section, the notations, some basic concepts and problem formulation are presented.

### A. Notation

First of all, some basic notations are given. The swarm is divided into  $N$  groups and each group is denoted by  $B_k$  ( $k = 1, \dots, N$ ).  $\alpha_i^{B_k}$  ( $i = 1, \dots, n$ ) and  $\alpha_l^{B_k}$  represent the  $i$ th UAV and the Co-leader in group  $B_k$ , respectively;  $n$  is the number of follower in each group;  $q_i^{B_k}$ ,  $p_i^{B_k}$ , and  $u_i^{B_k}$  represent the position, speed, and the control input of the corresponding UAV, respectively;  $N_l^{B_k}$  is the neighbor set of  $\alpha_l^{B_k}$ ;  $L$  is the

Laplace matrix; The symbol  $\otimes$  denotes the Kronecker product; the symbol  $\|\cdot\|$  denotes the 2-norm of a vector.

### B. Graph Theory

An undirected graph  $G = (V, \varepsilon)$  is used to describe the interaction among UAVs, which consists of a node set  $V = \{1, 2, \dots, (n+1)N\}$  and an edge set  $\varepsilon \subseteq V \times V$ . The edge  $(i, j) \in \varepsilon, i \neq j$  means that the  $\alpha_i^{B_k}$  can receive information from the  $\alpha_j^{B_k}$ . In this paper, assume that the underlying graphs are undirected and we have  $(i, j) \in \varepsilon \Leftrightarrow (j, i) \in \varepsilon$ . The formation is defined as  $(G, q^{B_k})$  which is a configuration  $q^{B_k}$  combining with a communication graph  $G$ .

### C. Modeling

In this paper, the model of UAVs can be considered as the second-order dynamical model, which can be expressed as

$$\begin{cases} \dot{q}^{B_k} = p^{B_k} \\ \dot{p}^{B_k} = u^{B_k} \end{cases} \quad (1)$$

In addition, to ensure the UAVs to gather, maintain a consistent speed, and avoid obstacles the following field function is introduced as

$$U(\|d\|) = \frac{k}{2} G (\|d\| - l)^2 \quad (2)$$

where,  $G$  is the constant of universal gravitation;  $U = [U_{mut}, U_{lea}, U_{obs}]^T$  is a set of potential field functions with different functions;  $d = [\bar{d}^T, \bar{d}^T, \bar{d}^T]^T$  and  $l = [\bar{l}^T, \bar{l}^T, \bar{l}^T]^T$  represent the actual distance and the desired distance, respectively;  $k = [\bar{k}, \bar{k}, \bar{k}]^T$  is the set of control coefficients.

Inspired by the flight characteristics of the birds flock, the standard configurations for the swarm like ellipses are constructed, which can refer to the block diagram a) in Fig. 1. During the swarm avoids obstacle, its surrounding neighbor can also dodge sideways when one UAV of the swarm detects an obstacle and avoids it, where their direction changes are transmitted layer by layer like ocean waves to pass through the entire swarm. The standard configuration of the swarm can be expressed as

$$\bar{l} = \left[ \left[ \left( \bar{l}_l^{B_1} \right), \left( \bar{l}_f^{B_1} \right) \right]^T, \dots, \left[ \left( \bar{l}_l^{B_k} \right), \left( \bar{l}_f^{B_k} \right) \right]^T \right]^T \quad (3)$$

where  $\bar{l}_f^{B_k} = \left[ (\bar{l}_1^{B_k})^T, \dots, (\bar{l}_n^{B_k})^T \right]^T$ ;  $\bar{l}_l^{B_k}$  is the desired distance between Co-leader  $\alpha_l^{B_k}$  and the swarm leader;  $\bar{l}_i^{B_k}$  is the desired distance between  $\alpha_i^{B_k}$  and its Co-leader  $\alpha_l^{B_k}$ .

### D. Problem formulation

Under the parallel control method, the swarm system of real world and virtual world (Virtual space domain and virtual time domain) are driven in parallel, where as the control variables in the virtual world are used to instruct the control quantity in the real world.

As shown in Fig. 2, to obtain the optimal control output for the swarm coordination ( $u$ ), the swarm system under the general configuration is mapped to the standard configuration

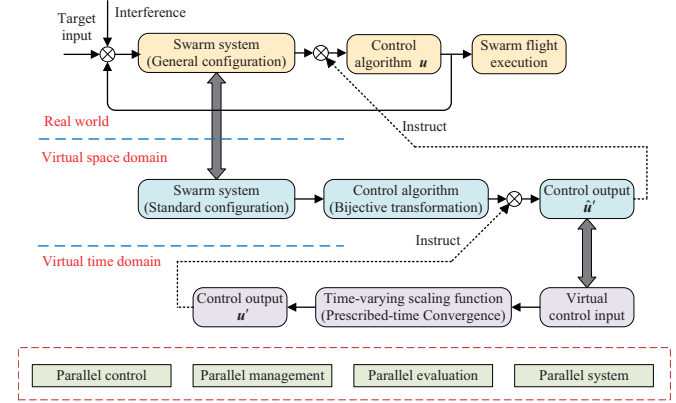


Fig. 2. Parallel control architecture of the swarm system.

of the virtual space domain through bijective transformation. Then, the corresponding control algorithm under the standard configuration ( $u'$ ) is designed to instruct the control output( $u$ ) in the real world.

To realize the prescribed-time convergence of the swarm system, the control variables are mapped to the virtual time domain through the time-varying scaling function. The control variable ( $u'$ ) that realizes the gradual convergence of the swarm system in this virtual time domain is designed. Then, this control variable is passed through the asymmetric mapping back into the real world time domain to instruct the rate of swarm control convergence.

It is worth noting that in this system, all controls are driven in parallel, managed in parallel, and executed in parallel. Based on the above description, we can design the dynamic swarm optimization function as follows:

$$J = \sum_{k=1}^N \sum_{i=1}^n \left( \|q^{B_k} - q_d - \hat{d}_d\| \right) + \sum_{k=1}^N \sum_{i=1}^n \left( \|p^{B_k} - p_s\| \right) \quad (4)$$

where,  $q_d$  is the position of the target UAV that maintains relative position for  $\alpha_i^{B_k}$ ;  $\hat{d}_d$  is the relative desired distance between the target UAV and  $\alpha_i^{B_k}$ ;  $p_s$  is the speed of the swarm leader. Therefore, the control goal of this paper is

$$\lim_{t \rightarrow T_{pre}} J = J_{min} \quad (5)$$

When  $t \rightarrow T_{pre}$  and  $J$  gets its minimum value, the optimal swarm control performance is achieved. At this point, the swarm formation maintains the ideal configuration, and the speeds of all UAVs are the same.

## III. CONTROL ALGORITHM FOR THE SWARM

In this section, the control laws for the UAVs are designed and the prescribed-time convergence is introduced.

### A. Control rules of the swarm

For the swarm to reach the destination successfully, the following control rules are designed.

- 1) Swarm leader: Suppose the swarm leader is used to receive flight instructions, which can lead the swarm to fly to the target area;

- 2) Co-leader leader: The only leader in each group, which can form a standard formation by maintaining the desired position with the swarm leader. Besides, by adjusting the position of some Co-leaders, the whole swarm formation can be changed based on the bijective transformation;
- 3) Followers: Keep the desired distance with the corresponding Co-Leader;
- 4) Communication of the swarm: Co-leaders between different groups can communicate with each other, followers within one group can communicate with each other, and followers belonging to different groups cannot communicate with each other, which the UAV members of other groups are identified as obstacles.

### B. Control law for the swarm

#### 1) Swarm control design of the leaders:

*Lemma 1:* [48] (LaSalle's principle) Let  $L: \mathbb{R}^n \rightarrow \mathbb{R}$  be a locally positive definite function such that on the compact set  $\Omega_c = \{x \in \mathbb{R}^n : L(x) \leq C\}$  ( $C$  is a constant greater than 0). If  $\dot{L}(x) \leq 0$  is satisfied, then where

$$S = \{x \in \Omega_c : \dot{L}(x) = 0\} \quad (6)$$

As  $t \rightarrow \infty$ , the trajectory tends to the largest invariant set inside  $S$ . In particular, if  $S$  contains no invariant sets other than  $x = 0$ , then 0 is an only equilibrium point.

Based on the above control rules of the swarm, the control laws of the Co-leaders can be designed as

$$\begin{aligned} \mathbf{u}_l^{B_k} = & - \sum_{j \in N_l^{B_k}} \hat{\mathbf{k}} \triangledown U_{mut} (\|\hat{\mathbf{d}}_{B_{ki,kj}}\|) \\ & - \bar{\mathbf{k}} \triangledown U_{lea} (\|\bar{\mathbf{d}}_l^{B_k}\|) \\ & - \sum_{m=1}^{\bar{m}} \tilde{\mathbf{k}} \triangledown U_{obs} (\|\tilde{\mathbf{d}}_{lo_m}^{B_k}\|) - b_1 \dot{\mathbf{q}}_l^{B_k} \\ & + \sum_{j \in N_l^{B_k}} a_{B_{ki,kj}}(t) \mathbf{p}_l^{B_{kj,ki}} \end{aligned} \quad (7)$$

where  $\mathbf{p}_l^{B_{kj,ki}} = \mathbf{p}_l^{B_{kj}} - \mathbf{p}_l^{B_{ki}}$ ;  $ki$  and  $kj$  are the positive integers representing the numbers of different groups;  $b_1$  is a control coefficient greater than 0.

#### 2) Analysis of the leader system stability:

*Theorem 1:* Consider a swarm leader system composed of  $N$  UAVs with the characteristics of Eq. (1). Under the control law of Eq. (7), the Co-leaders can converge to the standard formation without collisions occurring between the  $\alpha_l^{B_k}$  and other UAVs during their flying process.

*Proof:* To prove the system stability of the Co-leaders, the candidate Lyapunov function is set as

$$\begin{aligned} V_{co} = & \sum_{k=1}^N \left[ \sum_{j \in N_l^{B_k}} V_{mut} + V_{lea} + \sum_{m=1}^{\bar{m}} V_{obs} \right] \\ & + \frac{1}{2} \sum_{k=1}^N \|\dot{\mathbf{q}}_l^{B_k}\|^2 \end{aligned} \quad (8)$$

where,

$$V_{mut} = \frac{\hat{\mathbf{k}}}{2} G \left[ \sum_{j \in N_l^{B_k}} (\|\hat{\mathbf{d}}_{B_{ki,kj}}\| - \hat{l}_{B_{ki,kj}})^2 \right] \quad (9)$$

$$V_{lea} = \frac{\bar{\mathbf{k}}}{2} G (\|\bar{\mathbf{d}}_l^{B_k}\| - \bar{l}_l^{B_k})^2 \quad (10)$$

$$V_{obs} = \frac{\tilde{\mathbf{k}}}{2} G \left[ \sum_{m=1}^{\bar{m}} (\|\tilde{\mathbf{d}}_{lo_m}^{B_k}\| - \tilde{l}_l^{B_k})^2 \right] \quad (11)$$

where,  $V_{mut}$  represents the energy function of the interaction force between UAVs;  $\hat{\mathbf{d}}_{B_{ki,kj}}$  is the distance between two adjacent UAVs; and  $\hat{l}_{B_{ki,kj}}$  is the desired distance between these two UAVs; When  $\hat{\mathbf{d}}_{B_{ki,kj}} > \hat{l}_{B_{ki,kj}}$ ,  $\alpha_l^{B_{ki}}$  attracts  $\alpha_l^{B_{kj}}$ ; When  $\hat{\mathbf{d}}_{B_{ki,kj}} \leq \hat{l}_{B_{ki,kj}}$ ,  $\alpha_l^{B_{ki}}$  excludes  $\alpha_l^{B_{kj}}$ ;  $V_{lea}$  represents the energy function of the pilot force on  $\alpha_l^{B_k}$  where  $\bar{\mathbf{d}}_l^{B_k}$  and  $\bar{l}_l^{B_k}$  are the actual and desired distance between  $\alpha_l^{B_k}$  and the swarm leader, respectively;  $V_{obs}$  is the energy function of the obstacle avoidance force of  $\alpha_l^{B_k}$ ;  $\tilde{\mathbf{d}}_{lo_m}^{B_k}$  is the distance between  $\alpha_l^{B_k}$  and the  $m$ th obstacle;  $\tilde{l}$  is the safe distance between the UAV and the obstacle; When  $\tilde{\mathbf{d}}_{lo_m}^{B_k} < \tilde{l}$ , there will be a repulsive force from the obstacle acting on  $\alpha_l^{B_k}$ .

Taking the time derivative of the candidate Lyapunov function of the Co-leaders  $V_{co}$  as

$$\dot{V}_{co} = \sum_{k=1}^N (\dot{\mathbf{q}}_l^{B_k})^T \left[ \sum_{j \in N_l^{B_k}} \frac{\partial V_{mut}}{\partial \mathbf{q}_l^{B_k}} + \frac{\partial V_{lea}}{\partial \mathbf{q}_l^{B_k}} \right] \\ + \sum_{m=1}^{\bar{m}} \frac{\partial V_{obs}}{\partial \mathbf{q}_l^{B_k}} + \ddot{\mathbf{q}}_l^{B_k} \quad (12)$$

where,

$$\begin{aligned} \frac{\partial V_{mut}}{\partial \mathbf{q}_l^{B_k}} = & \sum_{j \in N_l^{B_k}} \hat{\mathbf{k}} G (\hat{l}_{B_{ki,kj}} - \|\hat{\mathbf{d}}_{B_{ki,kj}}\|) \frac{\partial \|\hat{\mathbf{d}}_{B_{ki,kj}}\|}{\partial \mathbf{q}_l^{B_k}} \\ = & \hat{\mathbf{k}} \sum_{j \in N_l^{B_k}} \triangledown U_{mut} (\|\hat{\mathbf{d}}_{B_{ki,kj}}\|) \end{aligned} \quad (13)$$

$$\begin{aligned} \frac{\partial V_{lea}}{\partial \mathbf{q}_l^{B_k}} = & - \bar{\mathbf{k}} G (\|\bar{\mathbf{d}}_l^{B_k}\| - \bar{l}_l^{B_k}) \frac{\partial \|\bar{\mathbf{d}}_l^{B_k}\|}{\partial \mathbf{q}_l^{B_k}} \\ = & - \bar{\mathbf{k}} \triangledown U_{lea} (\|\bar{\mathbf{d}}_l^{B_k}\|) \end{aligned} \quad (14)$$

$$\begin{aligned} \frac{\partial V_{obs}}{\partial \mathbf{q}_l^{B_k}} = & - \sum_{m=1}^{\bar{m}} \tilde{\mathbf{k}} G (\|\tilde{\mathbf{d}}_{lo_m}^{B_k}\| - \tilde{l}_l^{B_k}) \frac{\partial \|\tilde{\mathbf{d}}_{lo_m}^{B_k}\|}{\partial \mathbf{q}_l^{B_k}} \\ = & - \tilde{\mathbf{k}} \sum_{m=1}^{\bar{m}} \triangledown U_{obs} (\|\tilde{\mathbf{d}}_{lo_m}^{B_k}\|) \end{aligned} \quad (15)$$

Substituting Eqs. (13) - (15) into Eq. (12) yields

$$\begin{aligned} \dot{V}_{co} = & \sum_{k=1}^N (\dot{\mathbf{q}}_l^{B_k})^T \left[ \sum_{j \in N_l^{B_k}} \hat{\mathbf{k}} \triangledown U_{mut} (\|\hat{\mathbf{d}}_{B_{ki,kj}}\|) \right. \\ & \left. + \bar{\mathbf{k}} \triangledown U_{lea} (\|\bar{\mathbf{d}}_l^{B_k}\|) \right. \\ & \left. + \tilde{\mathbf{k}} \sum_{m=1}^{\bar{m}} \triangledown U_{obs} (\|\tilde{\mathbf{d}}_{lo_m}^{B_k}\|) + \mathbf{u}_l^{B_k} \right] \\ = & - \sum_{k=1}^N (\dot{\mathbf{q}}_l^{B_k})^T \left( \sum_{j \in N_l^{B_k}} a_{B_{ki,kj}} \mathbf{p}_l^{B_{kj,ki}} - b_1 \dot{\mathbf{q}}_l^{B_k} \right) \end{aligned} \quad (16)$$

Then, Eq. (16) can be written in a matrix form as

$$\dot{V}_{co} = -(\mathbf{p}_l^{B_k})^T [(\mathbf{L}(t) + b_1 I_n') \otimes I_n] (\mathbf{p}_l^{B_k}) \quad (17)$$

where,  $I_n'$  and  $I_n$  are identity matrices. Considering  $\mathbf{L}$  to be a positive semidefinite matrix, thus, we have

$$-(\mathbf{p}_l^{B_k})^T [(\mathbf{L}(t) + b_1 I_n') \otimes I_n] (\mathbf{p}_l^{B_k}) \leq 0 \Leftrightarrow \dot{V}_{co} \leq 0 \quad (18)$$

Considering that the energy of swarm system is limited, it is easy to see

$$V_{co} \leq V_0 \quad (19)$$

where  $V_0$  is the initial energy of the swarm system, and  $V_0 = C$ . If and only if  $\mathbf{p}_l^{B_k} = 0$ , then  $\dot{V}_{co} = 0$ .

Combining Lemma 1 with Eq. (18), we can get that all leaders will converge to the maximum invariant set, when the group system reaches a steady state, namely

$$S = \{(\hat{\mathbf{q}}^\alpha, \hat{\mathbf{p}}^\alpha) : -(\hat{\mathbf{p}}^\alpha)^T [(\mathbf{L}(t) + c_4 I_n') \otimes I_n] (\hat{\mathbf{p}}^\alpha) = 0\} \quad (20)$$

Then, the following conclusions can be drawn: i) Each solution of the set in Eq. (20) tends to the largest invariant set, which means the leader system of the swarm achieves aggregation; ii) The speed of the co-leaders are the same as the swarm leader, which shows the leadership of the swarm has speed consistency; iii) No collision occurs: If there is a collision, the energy function of the UAV will tend to infinity, which is in contradiction with the positive invariant compact set. This completes the proof. ■

### 3) Swarm control design of the followers:

**Theorem 2:** Consider a swarm follower system composed of  $n \times N$  UAVs with the characteristics of Eq. (1). Under the control law of Eq. (21), the followers can converge to the standard configuration without collisions occurring between the  $\alpha_i^{B_k}$  and other UAVs during their flying process.

$$\begin{aligned} \mathbf{u}_i^{B_k} = & - \sum_{i=1, i \neq j}^n \nabla U_{mut} \left( \left\| \hat{\mathbf{d}}_{i,j}^{B_k} \right\| \right) \\ & - \nabla U_{lea} \left( \left\| \hat{\mathbf{d}}_i^{B_k} \right\| \right) \\ & - \sum_{m=1}^{\bar{m}} \nabla U_{obs} \left( \left\| \tilde{\mathbf{d}}_{i,o_m'}^{B_k} \right\| \right) - b_2 \dot{\mathbf{q}}_i^{B_k} \\ & + \sum_{j \in N_i^{B_k}} a_{i,j}^{B_k}(t) \mathbf{p}_{j,i}^{B_k} \end{aligned} \quad (21)$$

where  $\mathbf{p}_{j,i}^{B_k} = \mathbf{p}_j^{B_k} - \mathbf{p}_i^{B_k}$ ;  $\hat{\mathbf{d}}_{i,j}^{B_k}$  is the distance between two adjacent followers;  $\hat{\mathbf{d}}_i^{B_k}$  is the distance between  $\alpha_i^{B_k}$  and its co-leader;  $\tilde{\mathbf{d}}_{i,o_m'}^{B_k}$  is the distance between  $\alpha_i^{B_k}$  and the  $m$ 'th obstacle;

The proof process of Theorem 2 is similar to the Theorem 1 except the only change of some parameters. Therefore, the stability of the followers system remains unchanged and still converges. The candidate Lyapunov function of the followers  $V_f \leq 0$ . The specific proof process is omitted.

### C. Prescribed-time Convergence

1) *Prescribed Convergence Time control design:* To ensure the efficiency of swarm transformation, the prescribed-time convergence theory is introduced, which can preset the convergence time of the formation transformation. The control input of the swarm system can be expressed as

$$\mathbf{u} = \left[ \left[ \left( \mathbf{u}_l^{B_1} \right), \left( \mathbf{u}_f^{B_1} \right) \right]^T, \dots, \left[ \left( \mathbf{u}_l^{B_k} \right), \left( \mathbf{u}_f^{B_k} \right) \right]^T \right]^T \quad (22)$$

where  $\mathbf{u}_f^{B_k} = \left[ (\mathbf{u}_1^{B_k})^T, \dots, (\mathbf{u}_n^{B_k})^T \right]^T$ .

Combining with Eq. (22), the swarm system can be described as

$$\dot{\mathbf{q}} = \mathbf{f}(\mathbf{q}(t), \mathbf{u}(t), t) \quad (23)$$

Here, the initial state of the system is assumed as  $\mathbf{q}(t_0) = \mathbf{q}_0$ . Considering that the functions in Eq. (23) are all nonlinear, which means the model of the swarm system is a nonlinear time-varying system. To realize the prescribed-time convergence control of the system, the state equation of Eq. (23) will be linearized in the following.

The nonlinear function in Eq. (23) is expanded into a Taylor series in the field of the operating point  $(\mathbf{q}_0, \mathbf{u}_0, t)$ , which the terms of the quadratic and the higher orders than 2 are all omitted. In this case, the following equality holds

$$\begin{aligned} \mathbf{f}(\mathbf{q}, \mathbf{u}, t) = & \mathbf{f}(\mathbf{q}_0, \mathbf{u}_0, t) + \frac{\partial \mathbf{f}}{\partial \mathbf{q}^T} |_{\mathbf{q}_0, \mathbf{u}_0, t} \cdot \Delta \mathbf{q} \\ & + \frac{\partial \mathbf{f}}{\partial \mathbf{u}^T} |_{\mathbf{q}_0, \mathbf{u}_0, t} \cdot \Delta \mathbf{u} \end{aligned} \quad (24)$$

where,  $\Delta \mathbf{q} = \mathbf{q} - \mathbf{q}_0$ ,  $\Delta \mathbf{u} = \mathbf{u} - \mathbf{u}_0$ . Then, we have

$$\dot{\mathbf{q}} = \dot{\mathbf{q}}_0 + \Delta \dot{\mathbf{q}} \quad (25)$$

The following formula is satisfied at the working point

$$\dot{\mathbf{q}}_0 = \mathbf{f}(\mathbf{q}_0, \mathbf{u}_0, t) \quad (26)$$

Therefore, the state space equation linearized by small perturbation can be calculated as

$$\begin{aligned} \Delta \dot{\mathbf{q}} = & \frac{\partial \mathbf{f}}{\partial \mathbf{q}^T} |_{\mathbf{q}_0, \mathbf{u}_0} \cdot \Delta \mathbf{q} + \frac{\partial \mathbf{f}}{\partial \mathbf{u}^T} |_{\mathbf{q}_0, \mathbf{u}_0} \cdot \Delta \mathbf{u} \\ = & \mathbf{A}(t) \Delta \mathbf{q} + \mathbf{B}(t) \Delta \mathbf{u} \end{aligned} \quad (27)$$

where,

$$\mathbf{A}(t) = \frac{\partial \mathbf{f}}{\partial \mathbf{q}^T} |_{\mathbf{q}_0, \mathbf{u}_0} = \begin{bmatrix} \frac{\partial f_1}{\partial q_1} & \dots & \frac{\partial f_1}{\partial q_n} \\ \vdots & \ddots & \vdots \\ \frac{\partial f_n}{\partial q_1} & \dots & \frac{\partial f_n}{\partial q_n} \end{bmatrix}_{\mathbf{q}_0, \mathbf{u}_0, t} \quad (28)$$

$$\mathbf{B}(t) = \frac{\partial \mathbf{f}}{\partial \mathbf{u}^T} |_{\mathbf{q}_0, \mathbf{u}_0} = \begin{bmatrix} \frac{\partial f_1}{\partial u_1} & \dots & \frac{\partial f_1}{\partial u_n} \\ \vdots & \ddots & \vdots \\ \frac{\partial f_n}{\partial u_1} & \dots & \frac{\partial f_n}{\partial u_n} \end{bmatrix}_{\mathbf{q}_0, \mathbf{u}_0, t} \quad (29)$$

In this way, the linear system shown in Eq. (27) can replace the nonlinear system in Eq. (23) with sufficient accuracy, when the nonlinear system moves near the operating point.

It can be known from Theorem 1 and Theorem 2 that the swarm system in Eq. (27) is stable and asymptotically

convergent in the time domain space of  $t$ , that is, when  $t \rightarrow \infty$ , then  $\Delta\mathbf{q}(t) \rightarrow 0$ , and the system forms a standard configuration. To achieve prescribed-time convergence, the time  $t$  is transformed and the virtual time domain ( $\rho$ -domain) space is introduced.

Suppose there exists a time-varying scaling function

$$a(t) = \frac{a_0 t}{1 - \frac{t}{T_1}} \quad (30)$$

where,  $T_1$  is the predetermined convergence time;  $a_0$  is a constant greater than 0. Taking the derivative of time  $t$  on both sides of Eq. (30), we get

$$a'(t) = \frac{a_0}{\left(1 - \frac{t}{T_1}\right)^2} := \alpha(\rho) \quad (31)$$

Let  $\rho = a(t)$ , and we have  $t = a^{-1}(\rho)$  ( $a^{-1}(t)$  existed) and  $d\rho = a'(t)dt$ , which can be further written as

$$\frac{dt}{d\rho} = \frac{1}{a'(t)} = \frac{1}{\alpha(\rho)} \quad (32)$$

Since  $t$  and  $\rho$  have the following transformation relationship

$$t = \frac{\rho}{a_0 + \frac{\rho}{T_1}} \quad (33)$$

and combining Eq. (31), the expression of  $\alpha(\rho)$  can be rewritten as

$$\alpha(\rho) = \frac{da}{dt} = \frac{a_0}{\left(1 - \frac{t}{T_1}\right)^2} = \frac{a_0}{\left(1 - \frac{\rho}{a_0 T_1 + \rho}\right)^2} \geq 0 \quad (34)$$

It can be seen from Eq. (34), when  $t \in [0, \infty)$ , then  $\rho \in [0, T_1]$ . Converting the swarm system in Eq. (27) to the  $\rho$ -domain, we have

$$\begin{aligned} \Delta\dot{\mathbf{q}}(\rho) &= \frac{d\Delta\mathbf{q}}{d\rho} = \frac{d\Delta\mathbf{q}}{dt} \cdot \frac{dt}{d\rho} \\ &= \frac{1}{\alpha(\rho)} [\mathbf{A}(\rho)\Delta\mathbf{q} + \mathbf{B}(\rho)\Delta\mathbf{u}] \end{aligned} \quad (35)$$

From Eq. (35),  $\Delta\dot{\mathbf{q}}(\rho)$  can be obtained. Further, the control input  $\Delta\mathbf{u}(\rho)$  in the  $\rho$ -domain can be calculated, which can make the system asymptotically converge under the  $\rho$ -domain. Then, the new control input  $\mathbf{u}'$  under the  $t$ -domain can be obtained through the conversion relationship in Eq. (33), which can be expressed as

$$\mathbf{u}'(t) = \Delta\mathbf{u}\left(\frac{\rho}{a_0 + \frac{\rho}{T_1}}\right) \quad (36)$$

At this time, for the swarm system, when  $t = 0$  then  $\rho = 0$ ; when  $t = T_1$  then  $\rho = \infty$ . That is, the system will converge asymptotically when  $\rho \rightarrow \infty$  under the  $\rho$ -domain, which means that the system converges asymptotically under the  $t$ -domain when  $t \rightarrow T_1$  under the  $t$ -domain.

2) *Stability analysis*: Based on the analysis in the previous section, the following theorem can be obtained.

**Theorem 3:** Consider a swarm system composed of  $(n+1)N+1$  UAVs with the characteristics of Eq. (1), which consists  $N$  co-leaders and  $n \times N$  followers. The start time is  $T_0$  and the end time is  $T_e$ . Under the control law of  $\mathbf{u}'$ , the swarm can converge to the standard configuration at time

$T_{pre}$  ( $T_{pre} = T_e - T_0$ ) without collisions occurring among the UAVs during their flying process.

*Proof:* To prove that the formation system can form the standard configuration within time  $T_{pre}$ , that is, to prove that the state tracking error can converge to zero asymptotically in the  $\rho$ -domain. At this time, the Lyapunov function of the swarm  $V = V_{co} + V_f$  is selected. Then, differentiating both sides of the Lyapunov function of the swarm with respect to the variable  $\rho$  yields

$$\frac{dV}{d\rho} = \frac{dV}{dt} \cdot \frac{dt}{d\rho} = \frac{dV}{dt} \cdot \frac{1}{\alpha(\rho)} \quad (37)$$

It follows from Theorem 1 and Theorem 2 that  $\frac{dV}{dt} \leq 0$ . Since  $\frac{1}{\alpha(\rho)} > 0$  based on the result of Eq. (34). Therefore, we have  $\frac{dV}{d\rho} \leq 0$ . When  $\frac{dV}{d\rho} = 0$ , all UAVs have the same speed.

That is, the stability of the system converges asymptotically, which means the above-mentioned time domain transformation does not affect the original stability of the system. This completes the proof. ■

#### IV. TURNING CONTROL OF THE SWARM

To realize the turning of the swarm, the turn strategy and the control method based on the bijection transform are presented.

##### A. Turning strategy of the swarm

It is found that the turning of the flock tends to maintain its geometry in the ground reference frame, which can make the energy consumption of the flock is the least during the turning flight. At this time, the birds in the outer ring do not need to accelerate the turn to maintain the relative position with their lead birds.

Therefore, the specific turning process in this paper can be described as the swarm geometric center is turning at a certain angular velocity. To be specific, the transformation of the group shape can be realized by adjusting the relative positions among co-leaders and the swarm leader, and among co-leader and its followers. This completes the turning of the swarm. The specific transformation process can refer the swarm turn control in Fig. 1, which implementation is based on the bijective transformation.

To better describe this turning process, the turning angular velocity  $w_l^{B_k}$  of the swarm can be described as a piecewise function of time  $t$  according to the turning radius at different times as

$$w_l^{B_k} = \begin{cases} w_{r_1} & \text{if } t \in [t_{strat}^{r_1}, t_{end}^{r_1}] \\ \vdots & \vdots \\ w_{r_n} & \text{if } t \in [t_{strat}^{r_n}, t_{end}^{r_n}] \end{cases} \quad (38)$$

where,  $w_{r_n}$  represents the angular velocity when turning with  $R_n$ ;  $t_{strat}^{r_n}$  and  $t_{end}^{r_n}$  represent the start and end times of the process, respectively.

Taking the turning process in Fig. 3 as an example ( $R_{r_n} \neq R_{r_{(n+1)}}$ ), the expression of angular velocity is derived as follows. It is known from the geometric relationship that there is

$$\theta_1^{r_n} = \theta_2^{r_n} = \theta_3^{r_n} \quad (39)$$

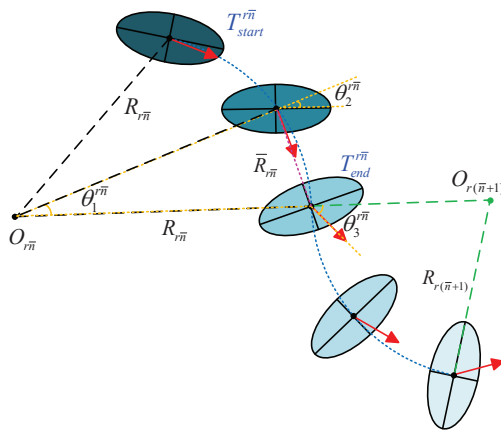


Fig. 3. Turning process of the swarm.

According to the cosine law, we can get

$$\cos(\theta_1^{r\bar{n}}) = \frac{R_{r\bar{n}}^2 + R_{r\bar{n}}^2 - \bar{R}_{r\bar{n}}^2}{2R_{r\bar{n}}^2} \quad (40)$$

where

$$\bar{R}_{r\bar{n}} = \left\| \mathbf{q}_l^{B_k}(t_{end}^{r\bar{n}}) - \mathbf{q}_l^{B_k}(t_{start}^{r\bar{n}}) \right\| \quad (41)$$

Then,  $\theta_1^{r\bar{n}}$  can be obtain via calculating  $\arccos(\theta_1^{r\bar{n}})$ . Considering that this geometric relationship exists for every segmented turn, the angular velocity of the geometric center can be generalized as

$$\omega_{r\bar{n}} = \frac{\theta_1^{r\bar{n}}}{T_{pre}^{r\bar{n}}} \quad (42)$$

where  $\theta_1^{r\bar{n}}$  is a turning angle of the turning with a turning radius of  $R_{r\bar{n}}$ ;  $T_{pre}^{r\bar{n}} = t_{end}^{r\bar{n}} - t_{start}^{r\bar{n}}$  is the predetermined convergence time of this turning process.

### B. Bijection transform

1) *Bijection transform control*: The configuration of the swarm before the change is defined as the general configuration, which is assumed that any two UAVs in this configuration are not collinear with the center of the configuration. And the standard configuration can refer to Eq. (3). The bijective transformation is to map the general configuration of the swarm to the standard configuration in the virtual space domain, then the force of the swarm control is designed, which can make the swarm form the desired formation in virtual space. After that, the control force can be mapped back to the real space via inverse transformation to form the desired configuration in real space.

Specifically, to realize the bijective transformation, a triangular region must be constructed, in which the position of the swarm leader is selected as the vertex, and the desired positions of the adjacent two UAVs are other two vertices of the triangular region. In this way, the space in the coordinate system can be divided into several triangular areas, and then the real coordinates can also be divided into several triangular areas correspondingly. As a result, the triangular space mapping control between the real and virtual coordinate system is constructed, which can realize the relative position

transformation between UAVs. Combined with the above, the following two lemmas are given.

**Lemma 2:** [49] There is a transformation matrix  $\mathbf{T}_i$  that can map the real coordinate system to the triangular space in the virtual coordinate system, which is a unique and invertible matrix and can be expressed as

$$\mathbf{T}_i = \tilde{\mathbf{T}}_i \cdot \mathbf{S} = \begin{bmatrix} a' & b' & c' \\ d' & e' & f' \\ 0 & 0 & 1 \end{bmatrix} \cdot \begin{bmatrix} \lambda & 0 & 0 \\ 0 & \lambda & 0 \\ 0 & 0 & 1 \end{bmatrix} \quad (43)$$

where,  $\tilde{\mathbf{T}}_i$  is the formation transformation matrix;  $\mathbf{S}$  is the scaling matrix, that is, the formation can be enlarged or reduced through  $\mathbf{S}$ , which is on the basis of keeping the geometric shape of the formation unchanged (when  $\lambda > 1$ , the formation shrinks; when  $\lambda < 1$ , the formation expands).

**Lemma 3:** [49] For a swarm system with  $(n+1)N+1$  UAVs, it can be divided into  $(n+1)N+1$  triangular regions, in which each triangular region has a unique reversible bijective transformation matrix in the real and virtual coordinate system, then the transformation matrix of the whole space is

$$\mathbf{T}_s = \begin{bmatrix} \mathbf{T}_1 & 0 & \cdots & 0 \\ 0 & \mathbf{T}_2 & \ddots & \vdots \\ \vdots & \ddots & \ddots & \vdots \\ 0 & \cdots & \cdots & \mathbf{T}_k \end{bmatrix} \quad (44)$$

### 2) Stability analysis:

**Theorem 4:** Consider a swarm system composed of  $(n+1)N+1$  UAVs with the characteristics of Eq. (1), under the control law of  $\hat{\mathbf{u}}'$ , the swarm can converge to the new desired formation within the time  $T_{pre}$  via changing the relative positions of the UAVs.

*Proof:* For the general configuration of the swarm, the following relationship between the virtual ( $\tilde{\mathbf{q}}'$ ) and the expected real coordinates ( $\tilde{\mathbf{q}}$ ) exists

$$\tilde{\mathbf{q}}' = \mathbf{T}_s \tilde{\mathbf{q}} \quad (45)$$

By substituting Eq. (45) into the control input  $\mathbf{u}'$ , we obtain the virtual control input of the swarm  $\tilde{\mathbf{u}}'$ . Further, the real control input  $\hat{\mathbf{u}}'$  after conversion can be expressed as

$$\hat{\mathbf{u}}' = \mathbf{T}_s^{-1} \tilde{\mathbf{u}}' \quad (46)$$

Considering that there is only a linear transformation relationship between the real and the virtual coordinates, which has no effect on the convergence of the original swarm system and the stability of the prescribed-time convergence system. Therefore, we have

$$\begin{aligned} \lim_{t \rightarrow T_{pre}} \mathbf{q}(t) &= \tilde{\mathbf{q}}(t) = \lim_{t \rightarrow T_{pre}} \mathbf{q}(\rho) \\ &= \lim_{t \rightarrow T_{pre}} \mathbf{T}_s^{-1} \tilde{\mathbf{q}}'(t) \\ &= \mathbf{T}_s^{-1} \tilde{\mathbf{q}}'(t) \end{aligned} \quad (47)$$

This completes the proof.  $\blacksquare$

## V. NUMERICAL SIMULATION

In this section, numerical simulations were presented to demonstrate the validity of the proposed control methods.

### A. Simulation parameters

In this simulation, the communication topology  $(G, \mathbf{q}^{B_k})$  among the swarm leader and Co-leaders can be seen the block diagram b) in Fig. 1, which lines indicate that the UAVs can communicate with each other. The communication structures of every group composed of the Co-leader and their followers are the same as  $(G, \mathbf{q}^{B_k})$ , which have no communication between different groups. The communication matrix of each group can be expressed as

$$\mathbf{L}^{B_k} = \begin{bmatrix} 6 & -1 & -1 & -1 & -1 & -1 & -1 \\ -1 & 3 & -1 & 0 & 0 & 0 & -1 \\ -1 & -1 & 3 & -1 & 0 & 0 & 0 \\ -1 & 0 & -1 & 3 & -1 & 0 & 0 \\ -1 & 0 & 0 & -1 & 3 & -1 & 0 \\ -1 & 0 & 0 & 0 & -1 & 3 & -1 \\ -1 & -1 & 0 & 0 & 0 & -1 & 3 \end{bmatrix} \quad (48)$$

A swarm of 43 UAVs were simulated as an example, which are divide the swarm into one swarm leader and 6 groups, and each group contains 1 co-leader and 6 followers. The relative position matrix of the standard configuration for each group can be expressed as

$$\mathbf{l}^{B_k} = \begin{bmatrix} -2 & -1 & -1 & 1 & 1 & 2 & 0 \\ 0 & -1 & 1 & -1 & 1 & 0 & 0 \end{bmatrix} \quad (49)$$

where the last column of the matrix is the relative position of the leader itself.

### B. Obstacle avoidance of the swarm

To show the ability of the swarm to avoid obstacles, a complete process of the formation composition, dissolution, transformation, reconstruction and maintain of the swarm was simulated. Fig. 4 is the trajectories of swarm obstacle avoidance, which shows the swarm has high maneuverability of changing the shape to avoid obstacles with no collision.

Fig. 5 are the tracking error curves, which are the relative errors of each UAV in 6 group in the whole process, respectively. To pass through the obstacle zone, the corresponding 4 stage actions were made by the swarm formation at time 0 s, 105 s, 220 s, 350 s, respectively. Taking into account factors such as flight distance and mission, each action was set to be executed within 105 s, 115 s, 130 s, and 80 s in turn. It can be observed from Fig. 5 that the UAVs can converge to zero within the prescribed time.

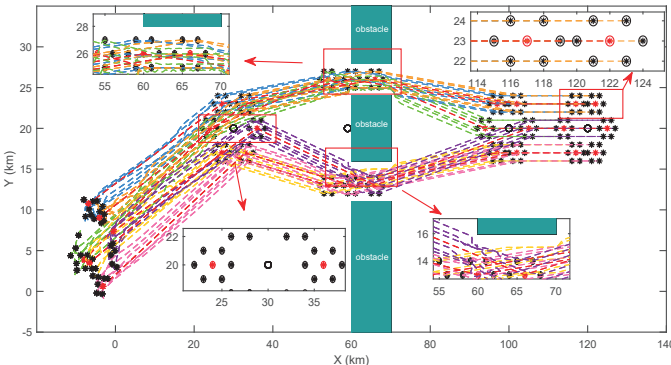


Fig. 4. Simulation of the obstacle avoidance for the swarm.

### C. Turning of the swarm

To show the ability of the swarm to turning, the turning process is artificially divided into 6 stages, and the turning radius is 20 km. Fig. 6 is the trajectories of swarm turning, which shows the swarm has high maneuverability of changing the shape to turning with no collision.

Fig. 7 are also the tracking error curves of 6 group, respectively. In simulation, the corresponding 6 stage actions were made by the swarm formation at time 0 s, 115 s, 160 s, 215 s, 240 s, and 255 s, respectively. And each action was set to be executed within 115 s, 45 s, 55 s, 25 s, 15 s and 50 s in turn. It is apparent from Fig. 7 that the UAVs can converge to zero within the prescribed time, which shows that the proposed turning method is more suitable for the swarm of large-scale UAVs.

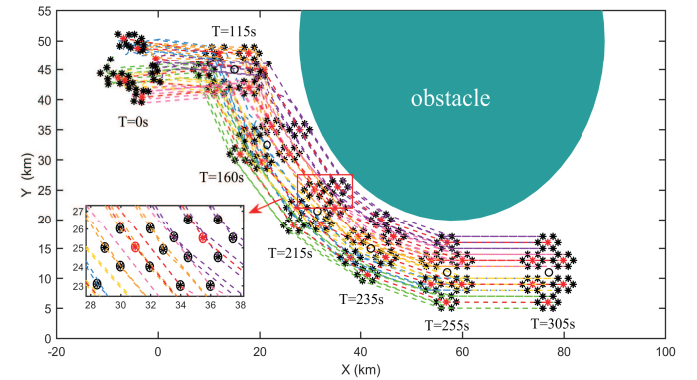


Fig. 6. Simulation of the turning for the swarm.

## VI. CONCLUSION

In this paper, we have proposed a parallel control method to realize the coordination of the swarm, which can make the UAVs achieve their expected changing positions within a prescribed time to obstacle avoidance and turning. Based on the leader-following structure, the swarm members can change the formation according to the actual situation, which is under the role of the potential field function and bijective transformation. In the meantime, the control laws were designed and analyzed, respectively, which shown the convergence time of the swarm system can be prescribed a prior no matter what conversion between the time domain and the space domain. The simulation results verified that the swarm can achieve large-scale coordination problem like turning and obstacle avoidance through efficient and rapid formation changes, which ensured the safety and stability flight of each UAV in the same time.

## REFERENCES

- [1] L. Tian, Y. Hua, X. Dong, J. Lv, and Z. Ren, "Distributed time-varying group formation tracking for multi-agent systems with switching interaction topologies via adaptive control protocols," *IEEE Trans. Ind. Informatics*, pp. 1–10, 2022.
- [2] D. Yu and C. L. P. Chen, "Automatic Leader-Follower Persistent Formation Generation with Minimum Agent-Movement in Various Switching Topologies," *IEEE Trans. Cybern.*, vol. 50, no. 4, pp. 1569–1581, 2020.
- [3] S. Wang et al., "Robotic Intra-Operative Ultrasound: Virtual Environments and Parallel Systems," *IEEE/CAA J. Autom. Sin.*, vol. 8, no. 5, pp. 1095–1106, 2021.

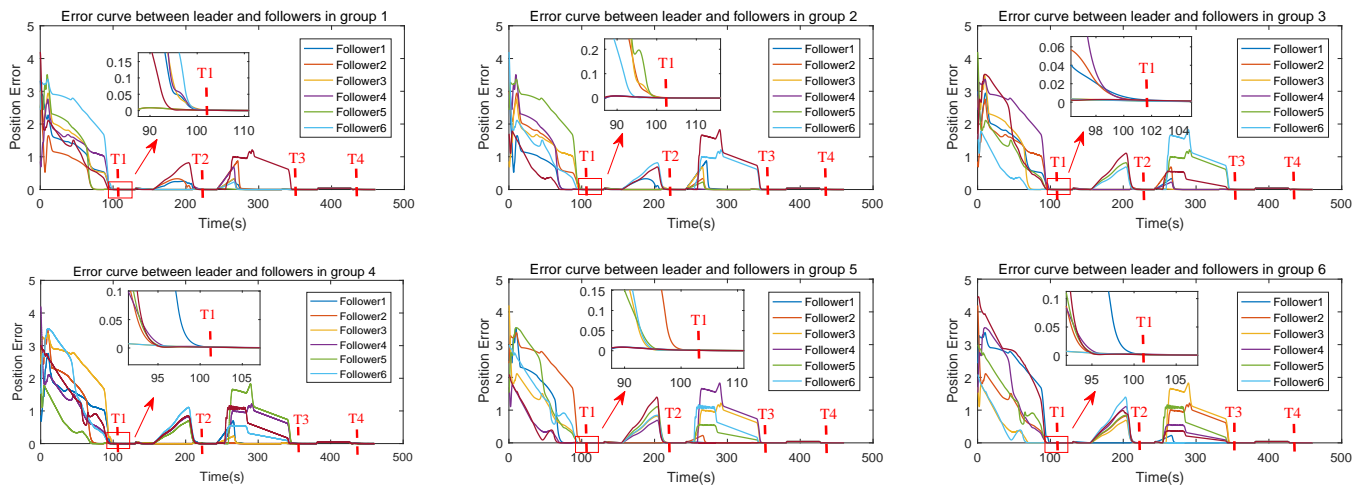


Fig. 5. Error curve between leader and followers in different groups.

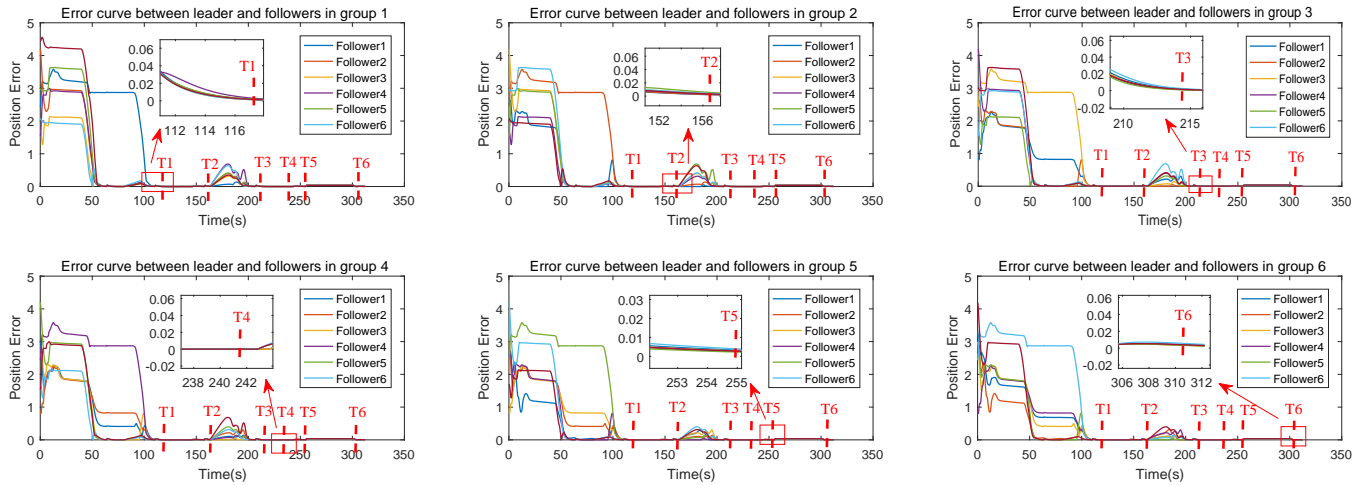


Fig. 7. Error curve between leader and followers in different groups.

- [4] D. Yu and C. L. P. Chen, "Smooth Transition in Communication for Swarm Control with Formation Change," *IEEE Trans. Ind. Informatics*, vol. 16, no. 11, pp. 6962–6971, 2020.
- [5] H. CHEN, X. WANG, L. SHEN, and Y. CONG, "Formation flight of fixed-wing UAV swarms: A group-based hierarchical approach," *Chinese J. Aeronaut.*, vol. 34, no. 2, pp. 504–515, 2020.
- [6] G. Luo, H. Zhang, H. He, J. Li, and F. Y. Wang, "Multiagent Adversarial Collaborative Learning via Mean-Field Theory," *IEEE Trans. Cybern.*, vol. 51, no. 10, pp. 4994–5007, 2021.
- [7] J. Wang, X. Ding, C. Wang, L. Liang, and H. Hu, "Affine formation control for multi-agent systems with prescribed convergence time," *J. Franklin Inst.*, vol. 358, no. 14, pp. 7055–7072, 2021.
- [8] X. Wang et al., "Coordinated flight control of miniature fixed-wing UAV swarms: methods and experiments," *Sci. China Inf. Sci.*, vol. 62, no. 11, pp. 1–17, 2019.
- [9] Z. J. Wang, Z. H. Zhan, S. Kwong, H. Jin, and J. Zhang, "Adaptive Granularity Learning Distributed Particle Swarm Optimization for Large-Scale Optimization," *IEEE Trans. Cybern.*, vol. 51, no. 3, pp. 1175–1188.
- [10] J. Fu, G. Wen, X. Yu, and Z.-G. Wu, "Distributed Formation Navigation of Constrained Second-Order Multiagent Systems With Collision Avoidance and Connectivity Maintenance," *IEEE Trans. Cybern.*, vol. 52, no. 4, pp. 1–14, 2020.
- [11] X. Li, Z. Xu, S. Li, Z. Su, and X. Zhou, "Simultaneous Obstacle Avoidance and Target Tracking of Multiple Wheeled Mobile Robots With Certified Safety," *IEEE Trans. Cybern.*, pp. 1–15, 2021.
- [12] J. Tang, S. Lao, and Y. Wan, "Systematic Review of Collision-Avoidance Approaches for Unmanned Aerial Vehicles," *IEEE Syst. J.*, pp. 1–12, 2021.
- [13] D. Yu, C. L. P. Chen, and H. Xu, "Fuzzy Swarm Control Based on Sliding-Mode Strategy with Self-Organized Omnidirectional Mobile Robots System," *IEEE Trans. Syst. Man, Cybern. Syst.*, vol. 52, no. 4, pp. 2262–2274, 2022.
- [14] H. Han, L. Zhang, X. Wu, and J. Qiao, "An efficient second-order algorithm for self-organizing fuzzy neural networks," *IEEE Trans. Cybern.*, vol. 49, no. 1, pp. 14–26, 2019.
- [15] Z. Pan, C. Zhang, Y. Xia, H. Xiong, and X. Shao, "An Improved Artificial Potential Field Method for Path Planning and Formation Control of the Multi-UAV Systems," *IEEE Trans. Circuits Syst. II Express Briefs*, vol. 7747, no. c, pp. 1–1, 2021.
- [16] W. Xu, L. Xiang, T. Zhang, M. Pan, and Z. Han, "Cooperative Control of Physical Collision and Transmission Power for UAV Swarm: A Dual-Fields Enabled Approach," *IEEE Internet Things J.*, vol. 9, no. 3, pp. 2390–2403, 2022.
- [17] J. Wu, C. Luo, Y. Luo, and K. Li, "Distributed UAV Swarm Formation and Collision Avoidance Strategies Over Fixed and Switching Topologies," *IEEE Trans. Cybern.*, pp. 1–11, 2021.
- [18] F. Venturini et al., "Distributed Reinforcement Learning for Flexible and Efficient UAV Swarm Control," *IEEE Trans. Cogn. Commun. Netw.*, vol. 7, no. 3, pp. 955–969, 2021.
- [19] L. Luo, X. Wang, J. Ma, and Y. S. Ong, "GrpAvoid: Multigroup Collision-Avoidance Control and Optimization for UAV Swarm," *IEEE*

- Trans. Cybern.*, pp. 1–14, 2021.
- [20] S. Tong, X. Min, and Y. Li, “Observer-Based Adaptive Fuzzy Tracking Control for Strict-Feedback Nonlinear Systems with Unknown Control Gain Functions,” *IEEE Trans. Cybern.*, vol. 50, no. 9, pp. 3903–3913, 2020.
- [21] Y. Yang, Y. Xiao, and T. Li, “Attacks on Formation Control for Multiagent Systems,” *IEEE Trans. Cybern.*, pp. 1–13, 2021.
- [22] D. Yu, C. L. P. Chen, and H. Xu, “Intelligent Decision Making and Bionic Movement Control of Self-Organized Swarm,” *IEEE Trans. Ind. Electron.*, vol. 68, no. 7, pp. 6369–6378, 2021.
- [23] C. Yang, C. Chen, W. He, R. Cui, and Z. Li, “Robot Learning System Based on Adaptive Neural Control and Dynamic Movement Primitives,” *IEEE Trans. Neural Networks Learn. Syst.*, vol. 30, no. 3, pp. 777–787, 2019.
- [24] X. Li, G. Qi, and L. Zhang, “Time-varying formation dynamics modeling and constrained trajectory optimization of multi-quadrotor UAVs,” *Nonlinear Dyn.*, vol. 106, no. 4, pp. 3265–3284, 2021.
- [25] X. Duan, Y. Zhou, D. Tian, J. Zhou, Z. Sheng, and X. Shen, “Weighted Energy Efficiency Maximization for a UAV-Assisted Multi-Platoon Mobile Edge Computing System,” *IEEE Internet Things J.*, pp. 1–1, 2022.
- [26] H. Li, Y. Wu, M. Chen, and R. Lu, “Adaptive Multigradient Recursive Reinforcement Learning Event-Triggered Tracking Control for Multiagent Systems,” *IEEE Trans. Neural Networks Learn. Syst.*, pp. 1–14, 2021.
- [27] Y. Yang, Y. Xiao, and T. Li, “A Survey of Autonomous Underwater Vehicle Formation: Performance, Formation Control, and Communication Capability,” *IEEE Commun. Surv. Tutorials*, vol. 23, no. 2, pp. 815–841, 2021.
- [28] N. Jung, B. M. Weon, and P. Kim, “Effects of adaptive acceleration response of birds on collective behaviors,” *J. Phys. Complex.*, vol. 3, no. 1, p. 15, 2022.
- [29] E. Cristiani, M. Menci, M. Papi, and L. Brafman, “An all-leader agent-based model for turning and flocking birds,” *J. Math. Biol.*, vol. 83, no. 4, pp. 1–22, 2021.
- [30] Y. Cao, J. Cao, and Y. Song, “Practical Prescribed Time Control of Euler-Lagrange Systems With Partial/Full State Constraints: A Settling Time Regulator-Based Approach,” *IEEE Trans. Cybern.*, pp. 1–10, 2021.
- [31] Y. Hua, X. Dong, Q. Li, and Z. Ren, “Distributed Fault-Tolerant Time-Varying Formation Control for Second-Order Multi-Agent Systems with Actuator Failures and Directed Topologies,” *IEEE Trans. Circuits Syst. II Express Briefs*, vol. 65, no. 6, pp. 774–778, 2018.
- [32] Y. Li, K. Li, and S. Tong, “Adaptive Neural Network Finite-Time Control for Multi-Input and Multi-Output Nonlinear Systems with Positive Powers of Odd Rational Numbers,” *IEEE Trans. Neural Networks Learn. Syst.*, vol. 31, no. 7, pp. 2532–2543, 2020.
- [33] Y. Hua, X. Dong, Q. Li, and Z. Ren, “Distributed fault-tolerant time-varying formation control for high-order linear multi-agent systems with actuator failures,” *ISA Trans.*, vol. 71, pp. 40–50, 2017.
- [34] L. Liu, T. Gao, Y. J. Liu, S. Tong, C. L. P. Chen, and L. Ma, “Time-varying IBLFs-based adaptive control of uncertain nonlinear systems with full state constraints,” *Automatica*, vol. 129, p. 109595, 2021.
- [35] Y. Yang, Y. Xiao, and T. Li, “Attacks on Formation Control for Multiagent Systems,” *IEEE Trans. Cybern.*, pp. 1–13, 2021.
- [36] Y. Li, K. Li, and S. Tong, “Adaptive Neural Network Finite-Time Control for Multi-Input and Multi-Output Nonlinear Systems with Positive Powers of Odd Rational Numbers,” *IEEE Trans. Neural Networks Learn. Syst.*, vol. 31, no. 7, pp. 2532–2543, 2020.
- [37] T. Xiong and Z. Gu, “Observer-based adaptive fixed-time formation control for multi-agent systems with unknown uncertainties,” *Neurocomputing*, vol. 423, pp. 506–517, 2021.
- [38] B. Liu, A. Li, Y. Guo, and C. Wang, “Adaptive distributed finite-time formation control for multi-UAVs under input saturation without collisions,” *Aerospace Sci. Technol.*, vol. 120, p. 107252, 2022.
- [39] Z. Wang, W. Fu, Y. Fang, S. Zhu, Z. Wu, and M. Wang, “Prescribed-time cooperative guidance law against maneuvering target based on leader-following strategy,” *ISA Trans.*, 2022.
- [40] X. Gong, Y. Cui, J. Shen, J. Xiong, and T. Huang, “Distributed Optimization in Prescribed-Time: Theory and Experiment,” *IEEE Trans. Netw. Sci. Eng.*, vol. 9, no. 2, pp. 564–576, 2021.
- [41] D. Yu, C. L. P. Chen, C. E. Ren, and S. Sui, “Swarm Control for Self-Organized System with Fixed and Switching Topology,” *IEEE Trans. Cybern.*, vol. 50, no. 10, pp. 4481–4494, 2020.
- [42] C. Q. Zhu and L. Liu, “Robust Adaptive Fuzzy Control via State-Dependent Function for Nonlinear Stochastic Large-Scale Systems Subject to Dead Zones,” *Complexity*, 2021.
- [43] H. Han, X. Wu, L. Zhang, Y. Tian, and J. Qiao, “Self-organizing RBF neural network using an adaptive gradient multiobjective particle swarm optimization,” *IEEE Trans. Cybern.*, vol. 49, no. 1, pp. 69–82, 2019.
- [44] Q. Wei, L. Wang, J. Lu, and F. Y. Wang, “Discrete-Time Self-Learning Parallel Control,” *IEEE Trans. Syst. Man, Cybern. Syst.*, vol. 52, no. 1, pp. 192–204, 2022.
- [45] F. Y. Wang, “Parallel control and management for intelligent transportation systems: Concepts, architectures, and applications,” *IEEE Trans. Intell. Transp. Syst.*, vol. 11, no. 3, pp. 630–638, 2010.
- [46] Q. Wei, H. Li, and F. Y. Wang, “A Novel Parallel Control Method for Continuous-Time Linear Output Regulation With Disturbances,” *IEEE Trans. Cybern.*, pp. 1–11, 2021.
- [47] Q. Wei, H. Li, and F. Y. Wang, “Parallel control for continuous-time linear systems: A case study,” *IEEE/CAC J. Autom. Sin.*, vol. 7, no. 4, pp. 919–928, 2020.
- [48] J. Zhan and Z. Jiang, “Self-Triggered Mechanism in General Linear Multiagent Systems,” *IEEE Trans. Ind. Informatics*, vol. 15, no. 7, pp. 3987–3997, 2019.
- [49] L. Sabattini, C. Secchi, and C. Fantuzzi, “Arbitrarily shaped formations of mobile robots: Artificial potential fields and coordinate transformation,” *Auton. Robots*, vol. 30, no. 4, pp. 385–397, 2011.